

# Tidally Phased Emergence Events in a Strongly Tidal Estuary

LESLIE H. TAYLOR, SHAWN M. SHELLITO, HEATHER U. ABELLO, and PETER A. JUMARS\*

*Darling Marine Center, University of Maine, 193 Clark's Cove Road, Walpole, Maine 04573*

**ABSTRACT:** Acoustic backscatter from an active sonar system over a range of six frequencies between 265 kHz and 3 MHz in the tidally dominated Damariscotta River estuary, Maine, United States, revealed that the major emergence event of the night commenced on the first tidal deceleration after dark (3.5–4 h after local slack), irrespective of flow direction. Emergence traps identified the mysid shrimp, *Neomysis americana*, as the dominant migrator. Water-column-integrated, acoustically estimated biovolume at our 10-m deep study location increased by a factor of about 6 during these large events, entirely dominating the holoplanktonic contribution and likely being a major component in benthic-pelagic coupling. Application of the same algorithm used to locate this nighttime emergence revealed a parallel but considerably smaller daytime emergence event near the same phase of the tide. Daytime trap samples failed to recover the organisms responsible, but transmissometry rejected the alternative hypothesis that we observed resuspension events. We suspect, but have yet only weak evidence, that animals emerging in daylight are copepods rather than mysids.

## Introduction

Emergence is often conceived as a single nocturnal event comprising animals emerging at dusk, maintaining a relatively constant density in the water column through the night, then returning to the seabed at dawn. Our initial study (Abello et al. 2005) demonstrated that emergence in the macrotidal Damariscotta River estuary, Maine, United States, was more temporally and spatially complex. As in other studies (e.g., Wang and Dauvin 1994; Oishi and Saigusa 1997), Abello et al. observed a light-cued emergence event at dusk. Additional emergence events were often noticed with varied intensities and durations during a single night. The largest and longest often occurred well after dark. During these events, emergent animals dominated pelagic biomass, relative to midday abundances, by an order of magnitude.

We recorded acoustic backscatter in 12.5-cm depth bins either every 1 or 2 min. Although this system revealed nuances in timing that would be impossible to resolve with traditional sampling methods, night-to-night variations and the sheer volume of observations made it difficult to detect and categorize patterns by eye. After tracking several suspected patterns that eventually proved inconsistent between observers, we adopted an algorithmic approach. Once we could reproducibly determine starting times of these dense emergence events, it became apparent that they followed a tidal phasing. We were able consistently to resolve a large emergence event that began 3.5–4 h after local slack tide, on the first tidal deceleration after dark.

Tidally phased emergence behaviors are well documented in intertidal species (Aleheit and Naylor 1976; Borowsky 1980; Takahashi and Kawaguchi 1997; Lawrie and Raffaelli 1998), but they are much less well known in the subtidal. We suspect a circatidal rhythm of emergence because emergence times are better predicted from a smoothed tidal model than from local observations of either tidal height or tidal velocity. Two not necessarily mutually exclusive hypotheses are suggested for this phasing. One is that increased turbulence at and just after peak tidal velocity reduces predation risk from tactile predators. Another is that avoiding the fastest tidal flows and staying in the water column during reversal limits the risk of overdispersal out of preferred habitats.

## Materials and Methods

A six-frequency Tracor acoustic profiling system (TAPS-6 from BAE SYSTEMS, San Diego, California) was deployed in the Damariscotta River estuary from spring to fall of 2001 and 2002. The Damariscotta River estuary, located in mid coast Maine, is macrotidal, well mixed, and receives very little freshwater input (Abello et al. 2005). In many ways it is functionally more a shallow, fjord-like indentation of the coast than a river. Its tides are semidiurnal with mean velocities on the order of 25 cm s<sup>-1</sup> and a tidal range of 3 m (Mayer et al. 1996). Substratum in the study area is a sandy silt.

TAPS in our configuration used 265-, 420-, 720-, 1,100-, 1,850-, and 3,000-kHz transducers in a moored, inverted echo-sounder mode. TAPS was placed by divers in approximately 10 m of water 50–100 m from the pier at the Darling Marine Center of the University of Maine at Walpole, Maine. We deployed it in a metal frame, positioned so that all 6

\*Corresponding author; tele: 207/563-3146; fax: 207/563-3119; e-mail: jumars@maine.edu

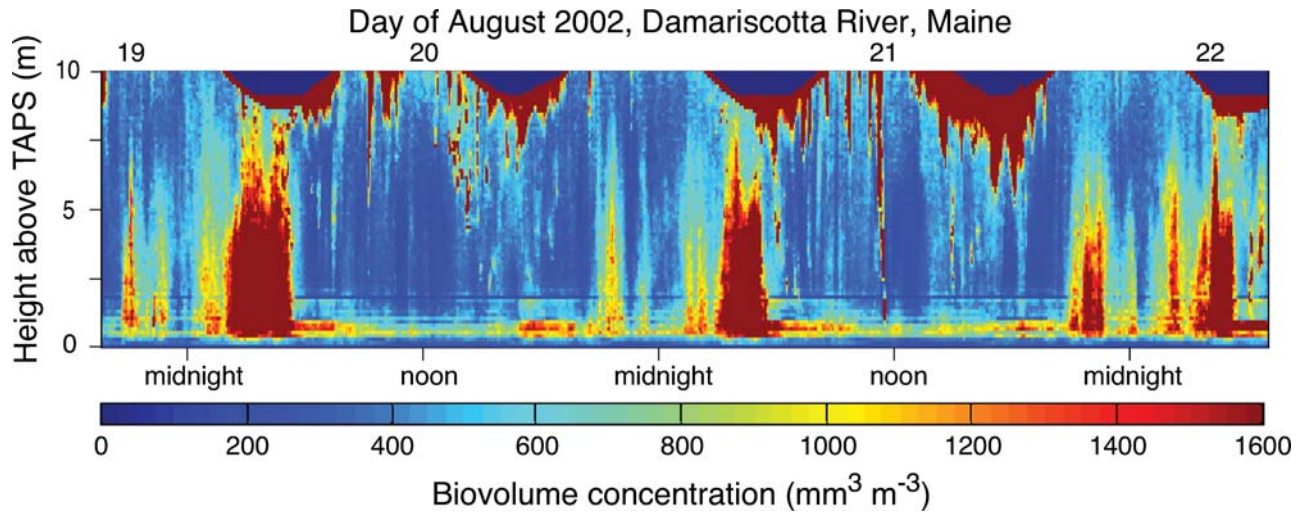


Fig. 1. Three days of biovolume profiles in August 2002. Note the multiple emergence events (upward-tapering sets of warm-colored pixels). The sea surface appears as a thick red band when the tide brings it < 10 m above bottom. Afternoon red pixels projecting down from the surface are from a combination of injected bubbles caused by whitecaps in afternoon seabreezes and near-surface fish schools (primarily juvenile alewives (*Alosa pseudoharengus*) at this season) that form nearshore during the day but disperse at night.

transducers were approximately 1 m above the substratum, facing upward. Power was supplied to TAPS from the pier through a 500-m, multi-conductor cable. For the data used here, once every minute each transducer of TAPS emitted 24 sets of high-frequency sonar pulses and measured backscatter from 12.5-cm range bins in the water column directly above TAPS. Pulse length was 336  $\mu\text{s}$  with 168  $\mu\text{s}$  between pulses. All 24 sets were then averaged at each frequency to produce a single output representing mean backscatter over 1 min for each depth bin, frequency, and minute. These data were transmitted through the cable to a laptop computer on the pier and recorded there.

We made extensive use of Matlab software (The Mathworks, Massachusetts) to process the voluminous acoustic data. Routines or M-Files are ASCII files written in the Matlab programming language and hereafter are specified as filename.m. All of them may be downloaded from <http://www.marine.maine.edu/~jumars/preprints/Appendix.pdf>. Multi-frequency inversion estimated volumetric abundance of scatterers (Holliday 1977, 1993; Greenlaw and Johnson 1983; McGehee et al. 1998). Using an equivalent spherical radius model (Greenlaw and Johnson 1982, 1983) and taking into account the temperature and salinity of the water (makets.m, invsndr.m; courtesy Charles Greenlaw, BAE SYSTEMS, San Diego, California), we inverted those smoothed backscatter data to biovolume ( $\text{mm}^3 \text{m}^{-3}$ ). For several reasons we did not resort to more complex inversions that involve elongate shapes. Spherical inversions are remarkably robust (when converted to equivalent volumes of the real body shapes involved; Greenlaw

and Johnson 1983; Pieper and Holliday 1984). Observed acoustic cross sections regress surprisingly well against biomass and even caloric content—not just biovolume (Benoit-Bird and Au 2002). Elongate-body models (e.g., McGehee et al. 1998) require observations or assumptions about animal orientation that we had little basis to make. Inversion based on spheres of equivalent volume yields an admittedly rough estimate of the total volume of particles likely to have produced the observed distribution of backscatter among frequencies. This total volume estimate will be called biovolume for the remainder of this paper, although it should be noted that the particles creating the backscatter used for the estimate are not necessarily living or even biogenic.

We restricted analysis of biovolume to the 24 range bins between 2 and 5 m above TAPS, i.e., 3–6 m above bottom. Nearer to TAPS, some of the frequencies were contaminated by ringing of the transducer and metal frame in response to the acoustic pulse. Further from TAPS, the highest frequencies gradually became range limited, restricting resolution of the smaller size classes.

Initial data processing followed the same procedures and used the same Matlab (Mathworks 1998) M-Files as did Abello et al. (2005). Local tide height was determined as the middle of the range bin with the highest mean backscatter intensity across frequencies (tideline.m). We processed raw backscatter voltages cumulated over the 24 pings for each depth bin, frequency, and time with the program makermt.m (Charles Greenlaw, BAE SYSTEMS) to calculate backscatter and used nospread.m to eliminate persistent vertical gradi-

ents that would interfere with the recognition of migration. Using an equivalent spherical radius model and taking into account the temperature and salinity of the water (makets.m, invsndr.m; Charles Greenlaw, BAE SYSTEMS), we inverted the processed backscatter data to biovolume ( $\text{mm}^3 \text{m}^{-3}$ ). For each range bin, we used only the sum of the biovolume across all size classes or total biovolume (Fig. 1). To create a one-dimensional time series, we summed over all the depths used to get a total biovolume within 3–6 m above the bottom.

Because multiple observers of data visualizations chose different events as major or minor and reported different start times, we devised an algorithm (findbigstart.m) to identify the longest-lasting, high-density emergence event and determine its start time. We applied the algorithm to half-day intervals denoted as nighttime (1,900–0,700 h) and daytime (0,700–1,900 h). We kept these search windows the same for all analyses even though day length changed through the season. For nocturnal emergence, we always wanted to search an interval that included times both before sunset and after sunrise. The algorithm uses both the magnitude and duration of biovolume increases to select only a single event for the time period searched (Fig. 2).

For a given interval, this algorithm searched each depth within the 3–6 m range above the seabed and identified times where measurements were above a threshold value in biovolume ( $\text{mm}^3 \text{m}^{-3}$ ). This threshold was free to vary from depth to depth and night to night. The algorithm first set an arbitrarily low threshold. If 240, not necessarily contiguous, observations (min) were above the selected value, the threshold was raised. Then the depth was searched again. The process repeated until  $< 240$  observations at each depth fell above the threshold. The threshold value used in the search algorithm crudely characterized an event's magnitude. We initially selected 240 observations as the cutoff because 240 min (4 h) matched the duration of discrete events that were boldly distinct from background levels. Both longer and shorter intervals produced less consistent results from night to night.

We defined any series of contiguous observations above threshold as an emergence event. The algorithm then identified the most pronounced emergence event by searching each depth for events of decreasing duration until an event of a given length was found in more than half of the depths. The initiation time of the largest emergence event was defined as the median time across depths of the first observation in the selected event (Fig. 2). Because above-threshold values were not continu-

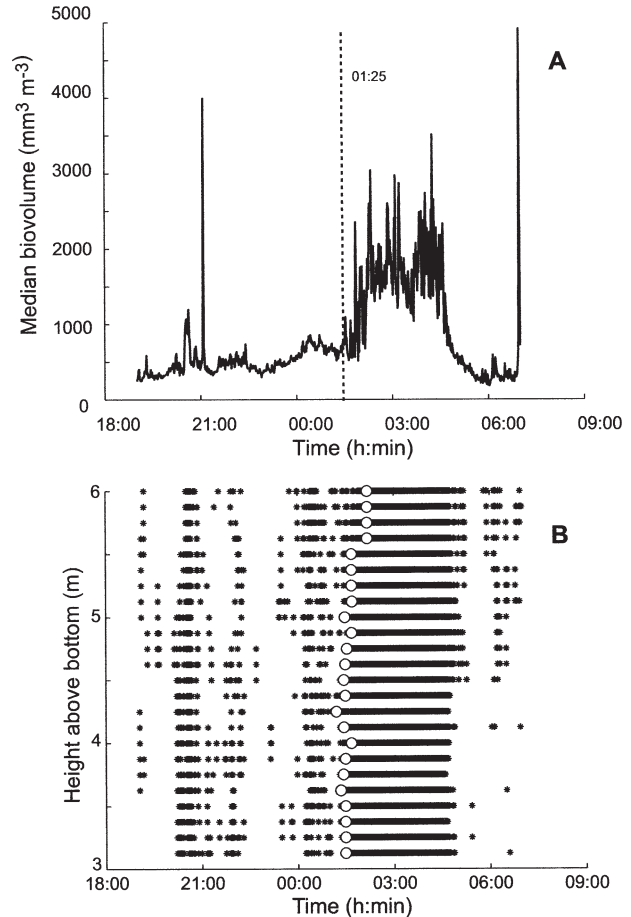


Fig. 2. Example of application of the algorithm that finds large events (findbigstart.m) to the first night in Fig. 1. A) Median biovolume over depth bins for the first night depicted in Fig. 1 (August 19–20, 2002). The dashed line indicates where the algorithm locates the start time of the major event. B) Asterisks indicate observations above the threshold at the indicated depth, and the open circles locate the algorithm-specified start time at that depth. The dashed line in panel A is the median time of the open circles in panel B.

ously present after onset of the large emergence event, the algorithm does not locate the termination of an event.

During the period of acoustic sampling in 2001 and 2002, four replicate emergence traps with 1-mm mesh sides covering 1 m<sup>2</sup> of seafloor (the same pyramidal design used by Kringel et al. 2003) were deployed in the area around TAPS an average of 4 times wk<sup>-1</sup>. Traps were usually deployed for approximately 24 h beginning around 1300 h EDT. Although the traps are not ideal, e.g., they change the flow regime above the sediment and may modify an animal's behavior, they provide baseline taxonomic and size information. In 2001 and the first part of 2002, two of the four traps were sealed at the bottom, whereas two were modified.

These modified traps were identical to the basic trap, but were elevated on steel legs 10 cm above the sediment. For the remainder of 2002, all four traps deployed were of the basic design (closed bottom). To reduce contamination with plankton, traps were lowered by hand with the base perpendicular to the seafloor, then pulled upright upon reaching bottom.

Acoustic observations often suggested several emergence events distributed throughout the night. To resolve whether these events represented multiple peaks of emergence by a single species or heterogeneity in emergence times among taxa or life stages, all four traps were also deployed for shorter periods during three consecutive days, August 19–22, 2002. Samples were collected and the traps redeployed near 0800, 1600, and again near 0000 h EDT daily.

Surface plankton tows were also performed both day and night. Collected specimens were fixed in 10% formalin, then transferred to 70% ethanol. All samples were archived, so that we could use measurements made on them to correlate with acoustic measurements and to detect seasonal changes in emergence behaviors and abundances. In a few samples, numbers of individuals of each species were counted. For the dominant species, *Neomysis americana*, individuals in those samples were also sorted by sex and developmental stage.

To obtain local current speeds near TAPS, an acoustic Doppler current profiler (Workhorse Series Monitor 600 kHz ADCP, RD Instruments, San Diego, California) was deployed. Like TAPS, the ADCP was connected through a multipurpose cable to a power supply and laptop computer on the pier. The ADCP was deployed on a steel frame that placed the transducers approximately 0.25 m above the sediment. The first bin recording velocities started at 1.22 m above bottom. We used 45 pings per 59.81-s ensemble. The ADCP measured the velocity in 10-cm vertical depth bins directly above it. ADCP velocity measurements were used to determine the offset between the time of a high or low tide at East Boothbay, Maine (as predicted by the online tide chart at <http://www.co-ops.nos.noaa.gov/tides04/tab2ec1a.html>), and local high and low tide. Velocity measurements were also used in cross correlation between bottom current speed and biovolume measurements.

Beam transmissometry was used to test the hypothesis that some apparent emergence events were instead backscatter from resuspended sediments. To the TAPS frame we mounted a WetLabs C-Star measuring transmission at 660 nm over a 10-cm path length, at the height of, but about 20 cm away from, the transducers.

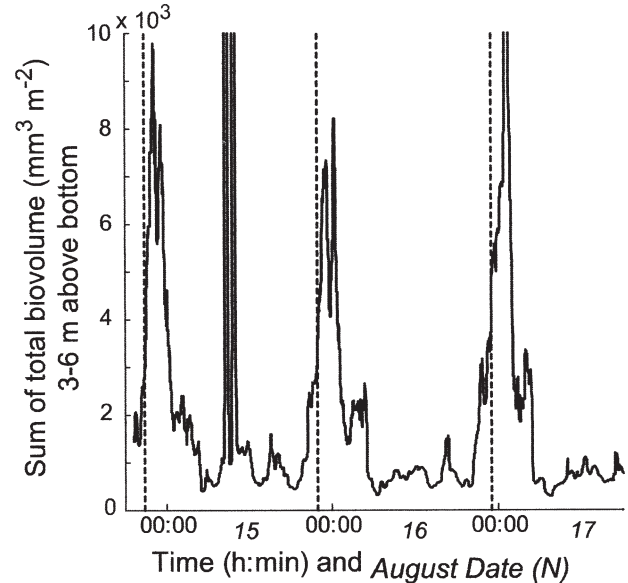


Fig. 3. During the large, nocturnal emergence events in August 2002, total water-column biomass estimates from 3 to 6 m above bottom were roughly 5.8 times their non-event, daytime values. Initiation times of events located through the algorithm (see text) are indicated by dashed lines. This time series began on August 14 and ended on August 17, 2002. The water column is about 3 times thicker than the layer used, so a rough correction would multiply the indicated totals by 3. Data were smoothed with a 19-point running median to reduce the number of spikes due to individual, large scatterers, but some spikes are still evident during the day on August 15.

We performed time-series analysis (Chatfield 1975) on depth-integrated biovolume data from August 1–22, 2002. We chose this interval because it held no data gaps. Time-series analysis was performed in Matlab (The Mathworks, Inc. 1984–2001, Massachusetts). Data were first detrended by subtracting a least-squares-fitted line (Matlab function `detrend`) prior to either autocorrelation or cross correlation.

To assess the contribution of emergence to total biovolume, we characterized central tendencies for biovolume data during emergence events and at times chosen to be fully outside emergence events. We first calculated the median biovolume measurement for 3–6 m above the sea floor. Then, to get a single, stable estimate insensitive to outliers, we found the median of the medians during the 2.5-h period immediately following the start time of each large daytime and large nighttime event. We repeated this procedure with 2.5-h long, non-event periods to obtain parallel estimates of vertically integrated biovolume.

## Results

TAPS showed multiple events per night (Fig. 1). The event identified by our magnitude-duration

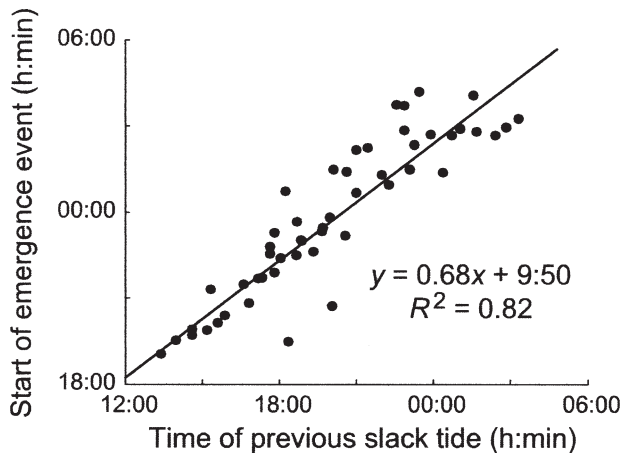


Fig. 4. For nocturnal observations in 2001 and 2002, there is a significant linear relationship between phase of the tide and initiation time of a high-density emergence event. A slope significantly lower than unity suggests that emergence is imperfectly in phase with the tides.

algorithm (Fig. 2) began during a specific tidal phase. It went in and out of phase with the light-cued events studied by Abello et al. (2005) because the M2 tides that dominate at our site are out of phase with the light cycle. Whereas the light-cued event always began near dusk, initiation time of the tidally-cued event shifted daily as times of high and low tide shifted. These large events showed dramatic increases of depth-integrated biovolume (Fig. 2). Emergence-trap samples indicated that the acoustic signal was dominated by the mysid shrimp *N. americana* and less so by the decapod shrimp *Crangon septemspinosa*. Emergence-trap samples from August 19–22 demonstrated that individuals of *N. americana* dominated both the emergence event (first of the night) detected by Abello et al. (2005) and the one reported here.

Nocturnal, high-density emergence events occurred on both incoming and outgoing tides. There was no significant difference in mean magnitude of emergence on incoming versus outgoing tides (983 and 952  $\text{mm}^3 \text{m}^{-3}$ , respectively, with standard deviations [SD] of 126 and 244  $\text{mm}^3 \text{m}^{-3}$ , respectively), even without correction for loss of degrees of freedom from using an autocorrelated time series. Least-squares, linear regression of emergence start time against time of local slack tide shows strong dependence (Fig. 4). The slope of the line is significantly below unity, which implies imperfect phasing with the tides. Closer inspection suggests that some of the disparity arises from emergence events near nightfall, where our algorithm likely fails to distinguish light-cued from tidally phased events, and indeed such events merge. A slope below unity implies a diminished lag between slack

tide and the initiation time of emergence when that slack tide occurs later at night. The implication is that if the optimal time of emergence based on tidal phase is too close to dawn, mysids emerge early, at slightly suboptimal tides, to ensure sufficient time in the water column.

Generally, high-density emergence began 3.5–4 h after local slack, when local tidal currents began their deceleration. Nocturnal high-density emergence events were better correlated with phase of the tide than with absolute local tidal current speeds. Although changes in tidal speed seemed to influence initiation of emergence, there appeared to be no threshold speed that triggered it: The mean current speed at 0.55–0.65 m above bottom at the start of a high-density emergence event varied widely from night to night (mean =  $14.9 \text{ cm s}^{-1}$ , SD =  $4.0 \text{ cm s}^{-1}$ ). Each night the current speed at the time of emergence represented a very common tidal current speed that was neither a maximum nor a minimum in the tidal cycle, making speed per se an unlikely cue.

We experimented with numerous algorithms that attempted to locate the end of the nighttime, large emergence event, e.g., by looking for series of various lengths below threshold. None proved consistently effective. When the large emergence event occurred shortly after dark, its end could sometimes be distinguished visually in our false-color plots from the dawn termination located by Abello et al. (2005). More often, termination of the large event was indistinguishable from the dawn reentry time located by Abello et al.'s much simpler algorithm based on relative rate of change of abundance. Very simply, the large nighttime event appeared most often terminated by the light cues discussed by Abello et al. (2005) rather than by tides, contributing to the ‘‘Dracula effect’’ (Abello et al. 2005, Fig. 9 and p. 495).

Although emergence has generally been conceived as an event or series of events occurring after dark, the close relationship between tidal phase and initiation of the major emergence event provoked questions about the pattern of backscatter at the same phase of the tide during the day. Applying the emergence algorithm to daytime observations highlighted an emergence-like event during the day near the same phase of the tide as the preceding night's emergence event (Fig. 5). Magnitudes of daytime events were substantially smaller (max  $550 \text{ mm}^3 \text{m}^{-3}$ ) than of events occurring at night (max  $1,600 \text{ mm}^3 \text{m}^{-3}$ ). During day, as well as night, there was a significant linear relationship between phase of the tide and initiation time of a backscatter event as detected by the emergence algorithm (Fig. 6). The slope of 0.75 is not significantly different from unity. When both night

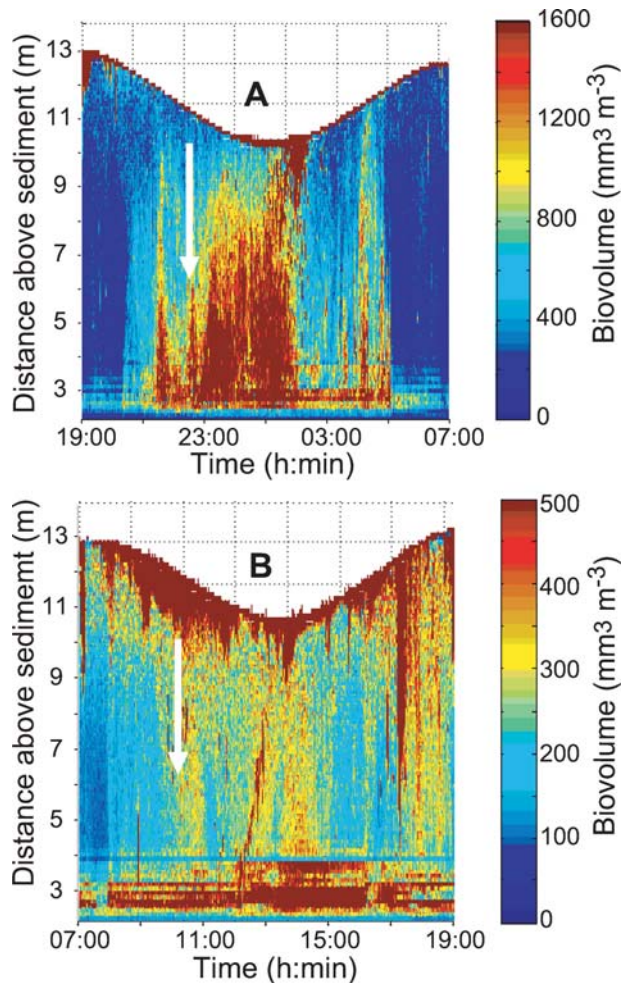


Fig. 5. The large nocturnal event (A) began at the time marked by the white arrow. A smaller increase in backscatter was located by the same algorithm and occurred near the same tidal phase the following day (B, white arrow). The time depicted in both panels as 0700 is August 17, 2002. Note the change in color scales, chosen to enhance contrast for the emergence events of interest. Dark red pixels near the surface represent high backscatter from the air-water interface, from bubbles injected by waves (in this season due largely to sea breezes) and from fishes (largely juvenile alewives, *Alosa pseudoharengus*) that school at the surface nearshore during daylight in this season.

and day are plotted together (Fig. 7), the slope is 0.96 and the intercept is 3.83 h (3:50), strongly supporting a common, tidal phasing.

The autocorrelogram of total, depth-integrated biovolume (3–6 m above bottom) showed coherence over 2-h intervals (Fig. 8a). At lags between 21 and 26 h, significant autocorrelation also was found. This broad peak probably reflects correlations with both the light cycle (24-h period; Abello et al. 2005) and the tides (25.4-h period). Negative correlations at roughly 6-h and 18-h lags are expected because they are exactly out of phase with the tides that

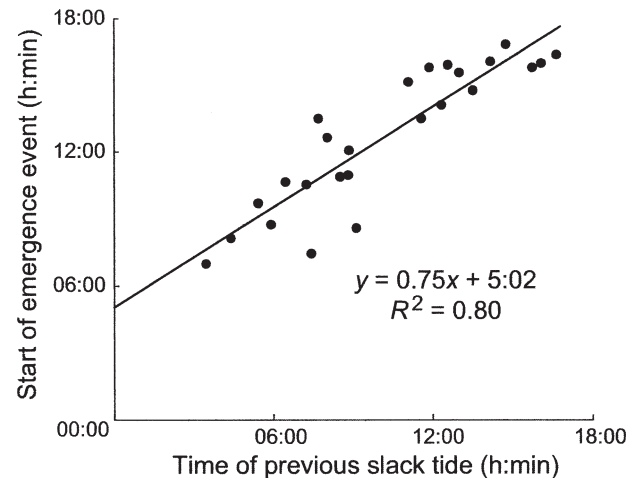


Fig. 6. For daytime observations in 2001 and 2002, there was a significant linear relationship between the phase of the tide and the time that a high-density emergence event begins. The slope was not significantly different from unity, so emergence may be in phase, on average, with the tides.

trigger emergence. This particular month and year happened to have an excess of emergence events on the outgoing tide due to its particular phasing of daylight and tides. Again, we chose this month for detailed analysis as the longest one for which we have continuous data every minute (approximately  $43 \times 10^3$  min). On a longer time scale, the autocorrelogram of total biovolume (3–6 m above bottom) showed autocorrelation at lags that are multiples of 25.4 h (Fig. 8b), weakening as expected with falling sample size at greater lags. The slight increases in peak heights near 13 d may reflect the

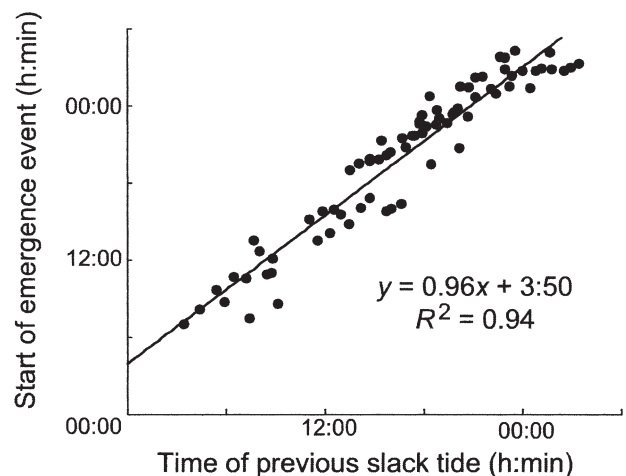


Fig. 7. When daytime and nighttime emergence events are plotted together, the slope of the relation between start times and times of the previous slack tide is very near unity, indicating a timing that is in phase with the tides and suggesting some adaptive value to this circatidal rhythm.

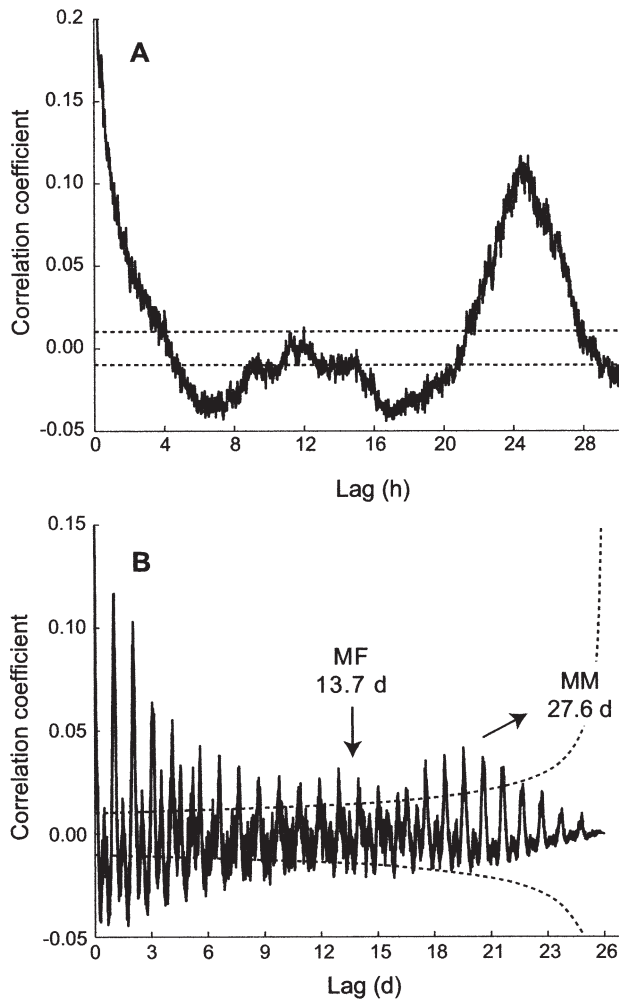


Fig. 8. Autocorrelogram of total, depth-integrated biovolume 3–6 m above bottom on the order of hours (A) shows coherence over about 4 h and a second, broad peak of positive autocorrelation from roughly 21–27 h. Negative autocorrelations at lags near 6 and 18 h result from dissimilarity of biovolume at opposing phases of the tide. The peak at 12 h fails to rise higher because of the dissimilarity in magnitude of daytime and nighttime emergence. On the time scale of days (B), harmonics of the 24-h peak are evident, and the taller peak at 12–14 d (lunar fortnightly period = MF) may be an indication of the spring-neap cycle. The second local maximum in peak height (base of arrow pointing toward MM, for the lunar monthly period) may indicate another increase in autocorrelation that is cut short by the finite length of record. Dashed lines are 95% confidence limits around the hypothesis of no significant autocorrelation.

period between two consecutive spring or neap tides and are near the limit of our resolution with a time series 23 d long. In this series as well as in others, emergent biovolume trended higher during spring tides than during neaps.

Depth-integrated biovolume and bottom tidal speed (Fig. 9a) showed significant positive cross correlation at lags of 0–3, 12–16, and 24–28 h and

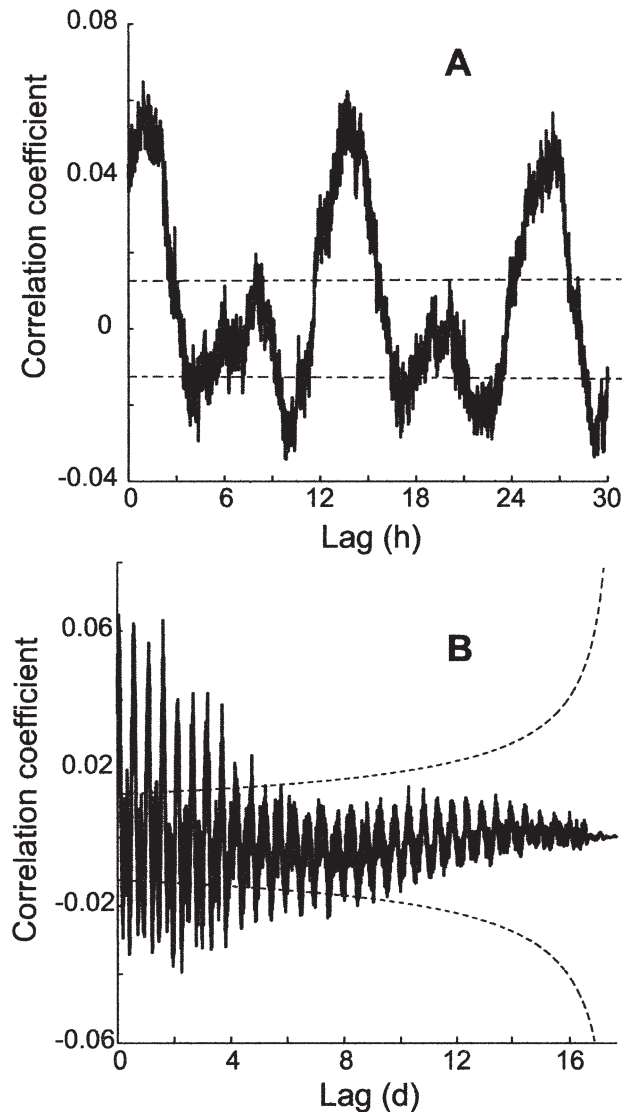


Fig. 9. Cross correlogram of total, depth-integrated 3–6 m biovolume and bottom tidal speed on the order of hours (A) shows significant positive cross correlations at lags between approximately 0–3, 11–15, and 24–28 h and significant negative cross correlation at lags of 4–5, 8–11, 17–18, and 20–23 h. The pattern is consistent with superimposed diel and tidal cycles but inconsistent with a diel cycle alone. Dashed lines indicate 95% confidence limits around the hypothesis of no significant cross correlation. The pattern of two positive cross correlation peaks per day persists on the order of days (B). The record hints at increased cross correlation at a lag of about 2 wk but is too short to have statistical power at this long lag, as the rapidly expanding confidence limits show.

significant negative cross correlation at lags of 3–6, 9–11, 17–18, and 20–23 h. These lags suggest that these two variables covary on a combination of tidal and diurnal cycles. Note that the absolute magnitude of the cross correlation coefficients (compounded across all events and non-events) is small

compared to the precision with which linear regression predicts the start time of an event. Cross correlation is less precise in predicting water-column biomass from phase of the tide than the regressions are in predicting start times of the large events. Whereas the onset of emergence corresponded with the beginning of tidal deceleration, peak abundances occurred substantially later. On a longer time scale (Fig. 9b), the pattern of two daily peaks of positive cross correlation persisted on the order of days.

In the continuous August record, we calculated (see Materials and Methods) a midday, non-event median of medians for depth-integrated biovolume of  $8,493 \text{ m}^3 \text{ m}^{-2}$ , whereas the nighttime, large-event median of medians was  $49,659 \text{ mm}^3 \text{ m}^{-2}$ . The large event represents a 5.8-fold increase in depth-integrated pelagic biovolume between these two periods. Parallel calculations using means were unstable because of their high sensitivity to large, individual scatterers during the day, likely fishes with swim bladders, that do not conform to the assumptions of the simple inversion model.

### Discussion

One of the problems with acoustic analysis is that backscatter patterns cannot yet be assigned to taxa (although doing so is an ultimate goal of acousticians). Supplemental sampling is required to determine what kinds of particles are responsible for the backscatter patterns detected acoustically. Nightly emergence trapping in the Damariscotta River estuary using pyramidal traps provided strong evidence that *N. americana* and *C. septemspinosa* emerge at night from mid July through the end of October. These species were the dominant constituents in all nocturnal trap samples that recovered emergent animals. In early July, when there was little evidence of emergence in the acoustic record, using emergence traps we captured few or no mysids. Nor did we catch mysids in nocturnal plankton tows at this time of year. Nocturnal plankton tows did capture mysids in surface waters at night at times when TAPS showed emergence.

Patchy mysid distributions on the seafloor (as routinely observed by divers servicing TAPS) and trapping artifacts make us reluctant to use trapped sample numbers as a direct analog to estimated biovolumes predicted by the inversions. Because emergence-trap samples measure the density of animals departing from a square meter of seafloor whereas TAPS estimates densities in the water column, it is difficult to make a direct comparison. We used trap and plankton-tow samples primarily as tools to identify what organisms participated in emergence events and what organisms were present

or absent in the water column at a given time of day or year.

Although we are quite confident that mysids are the primary contributors to the nocturnal data record, we are unsure what creates the emergence-like pattern in the daytime. Although we never caught mysids in traps or tows during the day, it is possible that mysids are responsible for both the diurnal and the nocturnal emergence. Mysids might emerge during the day but visually avoid entry into the trap funnel when there is light. Although trap avoidance selectively in daylight has never been documented, mysids are notorious for evading plankton nets (e.g., Clutter and Anraku 1968). It is possible that mysids with desperately low lipid stores might risk excursion into the water column during daylight.

Another hypothesis is that at least two participants create the pattern. One constituent emerges at a certain phase of tide, day and night. Only at night does the second constituent emerge in concert with the first. We initially hypothesized that one constituent was resuspended sediment. Transmissometry showed that beam attenuation, which is sensitive to scattering by small particles, in our study area a month after the emergence data analyzed here followed a diel rather than a tidal pattern, however, with maximal turbidity near or shortly after noon and a roughly linear decrease until the next morning. Further transmissometry in 2003 and 2004 has suggested more complex temporal structure of beam attenuation, but again no coincidence of high turbidity and start times of the large nighttime or parallel daytime events. At times of high tidal current speed, when one would expect resuspension, there was no corresponding increase in beam attenuation. We are continuing to pursue potential multiple relationships between suspended material and mysid activities, e.g., through both resuspension (Roast et al. 2004) and clearance by mysids (Sato unpublished data).

It may be that benthic copepods emerge both day and night but are accompanied or followed by emerging mysids during the night. We do find copepod parts frequently among mysid gut contents. Our traps have a mesh size of 1 mm, however, so we would have missed most emerging copepods. One problem with this hypothesis is that, whereas the daytime emergence pattern appears more convincing in the high-frequency channels that resolve smaller organisms, it is also weakly present in the 265-kHz channel that should be insensitive to copepod-sized organisms unless the copepod clouds are extremely dense (and hence violate the assumption of little multiple scattering that is needed for the inversion). We have some evidence from a summer Research Experience for Undergraduates

project using traps and plankton tows that a cyclo-poid copepod is associated with both the daytime and nighttime, tidally phased emergence events (Briggs personal communication). Further work is required to determine the role of copepod-sized organisms in the acoustic record of transducers at specific frequencies and to determine what is responsible for the unusual daytime, emergence-like acoustic signal.

At present, it is also unclear what makes a certain phase of tide a desirable time at which to initiate an emergence event or what cue (e.g., pressure, temperature, or some chemical cue) is used as the proximate one in tidal phasing. It is possible that animals select a time of decelerating tidal velocities in order to avoid the strongest tidal velocities that might result in the greatest displacement. The fact that the large event begins near a peak in tidal velocity suggests that animals may emerge at that time because of reduced risk of predation by tactile predators; high turbulence intensity may provide the mechanical analog of camouflage. The tidally phased events are also more abrupt than those cued by light (Abello et al. 2005), compatible with the idea of running a blockade of, or otherwise causing confusion in, predators. They are so abrupt that samples every minute cannot resolve a group ascent speed. Prominent predators of mysids, are the frequently trapped *C. septemspinusum*. Decelerating tidal currents also indicate the approach of slack tide and a directional change. With emergence of a few hours duration, an animal would spend some time traveling in one direction along the estuary, followed by some time traveling in the other, avoiding large net excursions from its point of departure.

Our results suggest that emergence in an environment with strong tidal velocities is richer in temporal structure than non-acoustic studies have been able to resolve. The existence of multiple emergence events by the same taxon leads one to ask why some individuals leave the seabed early in the evening while others wait. For taxa that migrate at multiple times we expect nutritional condition, as measured by lipid stores (cf., Hays et al. 2001), to correlate inversely with the risk of predation. We also expect nutritional state to decrease in order from the nighttime, tidally phased emergence to the dusk emergence, to the daytime emergence events. Mysids are important dietary components of many juvenile fishes. It will be informative in understanding benthic-pelagic coupling to understand the ways in which different kinds of emergence events regulate encounters between migrators, their prey, and their predators.

Whatever the cues, modulators, and consequences of emergence, acoustic data are raising

estimates of the apparent importance of emergence to nearshore pelagic ecology and benthic-pelagic coupling. Kringel et al. (2003) found a 14-fold increase in water-column integrated scattering strength during emergence events in a bay within Puget Sound, Washington, U.S. Here we found a 6-fold increase in water-column-integrated biovolume between midday and the large, tidally cued, nighttime events. More accurate estimates may require acoustic inversion that takes mysid body shapes and orientations into account, but the biovolume dominance of the large emergence event is indisputable. In view of their order-of-magnitude dominance in both places, it seems likely that mysids in the 1-cm size category have been under-sampled broadly by traditional means and certainly underresolved in space and time. Contributions of emergence to vertical fluxes of matter and energy and to fisheries food webs deserve enhanced attention.

#### ACKNOWLEDGMENTS

This work was supported by U.S. Office of Naval Research grants N00014-00-1-0662 and N00014-03-1-0776. We thank Charles Greenlaw and D. Van Holliday for help above and beyond the call of duty with hardware and software. Kelly Dorgan often assisted with diving tasks. Percy Donaghay and an anonymous reviewer provided useful suggestions that materially improved this paper. This paper summarizes the M.S. research of the first author.

#### LITERATURE CITED

- ABELLO, H. U., S. M. SHELLITO, L. H. TAYLOR, AND P. A. JUMARS. 2005. Light-cued emergence and reentry events in a strongly tidal estuary. *Estuaries* 28:487–499.
- ALHEIT, J. AND E. NAYLOR. 1976. Behavioural basis of intertidal zonation in *Eurydice pulchra* Leach. *Journal of Experimental Marine Biology and Ecology* 23:135–144.
- BENOIT-BIRD, K. J. AND W. W. L. AU. 2002. Energy: Converting from acoustic to biological resource units. *Journal of the Acoustical Society of America* 111:2070–2075.
- BOROWSKY, B. 1980. Factors that affect juvenile emergence in *Gammarus palustris*. *Journal of Experimental Marine Biology and Ecology* 42:213–223.
- CHATFIELD, C. 1975. *The Analysis of Time Series: Theory and Practice*. Chapman and Hall, London, U.K.
- CLUTTER, R. I. AND M. ANRAKU. 1968. Avoidance of samplers, p. 47–76. In D. J. Tranter and J. H. Fraser (eds.), *Zooplankton Sampling, Monographs on Oceanographic Methodology, Volume 2*. United Nations Educational, Scientific and Cultural Organization, Paris, France.
- GREENLAW, C. F. AND R. K. JOHNSON. 1982. Physical and acoustical properties of zooplankton. *Journal of the Acoustical Society of America* 72:1706–1710.
- GREENLAW, C. F. AND R. K. JOHNSON. 1983. Multiple-frequency acoustical estimation. *Biological Oceanography* 2:227–252.
- HAYS, G. C., H. KENNEDY, AND B. W. FROST. 2001. Individual variability in diel vertical migration of a marine copepod: Why some individuals remain at depth while others migrate. *Limnology and Oceanography* 46:2050–2054.
- HOLLIDAY, D. V. 1977. Extracting bio-physical information from the acoustic signatures of marine organisms, p. 619–624. In N. R. Andersen and B. J. Zahuranec (eds.), *Ocean Sound Scattering Prediction*. Plenum Press, New York.

- HOLLIDAY, D. V. 1993. Zooplankton acoustics, p. 733–740. In B. N. Desai (ed.), *Oceanography of the Indian Ocean*. A. A. Balkema, Rotterdam, Netherlands.
- KRINGEL, K., D. V. HOLLIDAY, AND P. A. JUMARS. 2003. A shallow scattering layer: High-resolution acoustic analysis of nocturnal vertical migration from the seabed. *Limnology and Oceanography* 48:1223–1334.
- LAWRIE, S. M. AND D. G. RAFFAELLI. 1998. In situ swimming behavior of the amphipod *Corophium volutator*. *Journal of Experimental Marine Biology and Ecology* 224:237–251.
- Mathworks. 1998. MATLAB: Signal Processing Toolbox. Mathworks, Natick, Massachusetts.
- MAYER, L. M., D. W. TOWNSEND, N. R. PETTIGREW, T. C. LODER, M. W. WONG, D. KISTNER-MORRIS, A. K. LAURSEN, A. D. SCHOUEDEL, C. CONAIRIS, J. BROWN, AND C. NEWELL. 1996. The Kennebec, Sheepscot and Damariscotta River estuaries: Seasonal oceanographic data. University of Maine, Department of Oceanography Technical Report #9601:1–110. Orono, Maine.
- MCGEHEE, D. E., R. L. O'DRISCOLL, AND L. V. MARTIN-TRAYKOVSKI. 1998. Effects of orientation on acoustic scattering from Antarctic krill at 120 kHz. *Deep-Sea Research II* 45:1273–1294.
- OISHI, K. AND M. SAIGUSA. 1997. Nighttime emergence patterns of planktonic and benthic crustaceans in a shallow subtidal environment. *Journal of Oceanography* 53:611–621.
- PIEPER, R. E. AND D. V. HOLLIDAY. 1984. Acoustic measurements of zooplankton distributions in the sea. *Journal du Conseil pour l'Exploration de la Mer* 41:226–238.
- ROAST, S. D., J. WIDDOWS, N. POPE, AND M. B. JONES. 2004. Sediment-biota interactions: Mysid feeding activity enhances water turbidity and sediment erodability. *Marine Ecology Progress Series* 128:145–154.
- TAKAHASHI, K. AND K. KAWAGUCHI. 1997. Diel and tidal migrations of the sand-burrowing mysids *Archaeomysis kokuboi*, *A. japonica*, and *Tiella oshimai*, in Otuschi Bay, northeastern Japan. *Marine Ecology Progress Series* 148:95–107.
- WANG, Z. AND J. C. DAUVIN. 1994. The suprabenthic crustacean fauna of the infralittoral fine sand community from the Bay of Seine (Eastern English Channel): Composition, swimming activity and diurnal variation. *Cahiers de Biologie Marine* 35:135–155.

#### SOURCES OF UNPUBLISHED MATERIALS

- BRIGGS, A. personal communication. P.O. Box 263, Bremen, Maine 04551.
- SATO, M. unpublished data. Darling Marine Center, University of Maine, 193 Clark's Cove Road, Walpole, Maine 04573.

*Received, November 30, 2004*

*Accepted, March 17, 2005*